

FIRE DETECTION AND LOCATION THROUGH INVERSE PROBLEM SOLUTION

by

**R.F. Richards and O.A. Plumb
Washington State University
Pullman, WA, USA**

International Conference on Fire Research and Engineering, September 10-15, 1995. Orlando, FL. Proceedings. Sponsored by National Institute of Standards and Technology (NIST) and Society of Fire Protection Engineers (SFPE). D. Peter Lund and Elizabeth A. Angell, Editors. Society of Fire Protection Engineers, Boston, MA, 1995.

NOTE: This paper is a contribution of the National Institute of Standards and Technology and is not subject to copyright.

Introduction

A prototype system which can detect, locate, and size an accidental fire within the first few minutes of the fire's ignition is presented. The prototype system employs a black and white video camera to monitor color-changing temperature sensitive sensors distributed around the space to be protected. Transient temperatures revealed by the sensors and gathered by the video camera are used as data to locate and size the fire in an algorithm based on the solution of an inverse heat transfer problem. Limits on the accuracy of the inverse problem solution algorithm, both in locating fires and determining their heat release rate are established using computer synthesized fire data. The validity of the computer simulations is verified with results of experimental tests of the prototype detection system in locating and sizing flame sources in a lab scale enclosure.

Inverse Problem Solution Algorithm

The problem of locating a fire and determining its growth rate can be formally posed as an inverse problem¹. In the present study the problem is taken to be one of parameter estimation in which three unknown parameters are to be found: x , y , and α . The location of the fire is described by the Cartesian coordinates, (x,y) , where the fire is assumed to lie in the plane of the compartment floor. The fire growth rate is determined by the parameter α , which follows from the functional form of the fire heat release rate assumed in the present work:

$$Q = \alpha t^2 \quad (1)$$

The quadratic form is chosen following Heskestad's recommendation² for the initial stages of fire growth. Here Q is the fire's convective heat release rate in kW, and t is the elapsed time from the ignition of the fire in seconds. The parameter to be found, α , is seen to have units of kW/s².

Solution of the inverse problem requires two steps: first prediction of the transient temperature field using a numerical fire model, and second minimization of the residuals between measured and predicted temperatures to determine the most probable location and heat release rate for the fire. The first step, determination of the temperature field given the heat source, is commonly referred to as solution of the forward problem. The second step, comparison of transient temperature data gathered by sensors to predictions of those temperatures by the numerical fire model to obtain location and heat release rate information about the fire, completes solution of the inverse problem.

In the present study the solution of the forward problem is found using the compartment fire model LAVENT. LAVENT, a two-zone fire model employing semi-empirical models of the buoyant plume and ceiling jet is able to compute convective heat fluxes from a fire to the ceiling of a compartment³. Forward problem solutions in the form of transient temperature fields are found for a set of many fire scenarios, each consisting of a fire with a given location and growth

rate, (x,y,α) , in the relevant compartment geometry. Using the transient temperature solution for each scenario, the times at which each sensor will be activated can be determined, given both the locations of the temperature-sensitive sensors and their activation temperature

The inverse problem solution algorithm can be applied to a fire of unknown location and growth rate, given data in the form of times at which individual sensors are activated as a result of the plume of hot gases rising from the fire. The inversion algorithm proceeds by subtracting measured times-to-activation from predicted times-to-activation and then summing the squares of the differences. The solution to the inverse problem is taken to be the values of the parameters x , y , and α for the fire scenario which minimizes the sum of squares of residuals over the complete set of fire scenarios

Prototype Fire Detection System

A prototype fire detection system has been assembled and set up in a model enclosure⁴. The prototype system consists of a 486 personal computer, a PULNEX TM-7CN black and white video camera, a SCENTECH IV-P24 frame grabber, and an array of color-changing sensors. The enclosure is 1 m high, 2.75 m wide and 2.75 m deep, with a ceiling made of 2.5 cm thick polystyrene foam. The side walls are open. Temperature-sensitive color-changing sensors, each 10 by 10 cm squares, are hung from the enclosure ceiling in a square grid, spaced one meter apart. Two types of sensors have been tested. Sensors have been fabricated from thermochromic liquid crystal sheets which display a color-play over a given temperature range, and sensors have been fabricated from wax based paints which liquify and clear at set temperatures.

The prototype system is able to monitor the TLC sensors on a nearly continuous basis. The personal computer commands the frame grabber to "grab" images from the black and white video camera, digitize the images and transfer the matrix of pixel values to the PC's RAM about once a second. Once in memory, the code compares the pixel values of each TLC sensor image with pixel values of a black "normalizing" surface located adjacent to the TLC sensor. Comparing changes in the TLC sensor with an unchanging "normalizing" surface enables the code to distinguish color changes in the TLC sensor from changes in sensor lighting.

If the code detects a color change in any TLC sensor, the location of the sensor and the time of the change (to the nearest second) are recorded. Upon the activation of five TLC sensors within a time span of five minutes a fire alarm is called. Once the alarm is called and a fire has been detected, the locations and times-to-activation of the five TLC sensors are transferred to the inverse problem solution algorithm to be used as data to locate and sized the fire.

Results

The performance of the inverse problem solution algorithm, on which the proposed fire detection system is based, was evaluated by simulating fires with known location and growth rate (x,y,α) in a compartment. Both systematic and random error was added to the computer simulated data following the model:

Simulated times-to-activation, $t_{sim,i}$ were then:

$$\hat{t}_{sim,i} = \hat{t}_{LAV,i} + (a + b\hat{t}_{LAV,i}) + G(\sigma) \quad (2)$$

where $t_{LAV,i}$ is the time-to-activation of the i th sensor as calculated by LAVENT, a and b are constants characterizing systematic error, and $G(\sigma)$ is a random number chosen from a normal

distribution with standard deviation σ . Note that the parameter a has units of seconds and represents a constant time bias, while the parameter b , which is dimensionless, represents a constant percentage error in elapsed time.

Sensor times-to-activation calculated for the simulated fires were then used as data for the inversion algorithm to reconstruct the location and heat release rate of the simulated fires. Results of the evaluation of the inverse problem solution algorithm for fire detection are given in Figs. 1 through 6. Two results are of particular interest in the present study: the speed with which the system can detect a fire, and the accuracy with which the inverse algorithm can locate and size the fire.

Figure 1 shows probability distribution functions (pdf's) for times-to-activation for the first and fifth sensors for a slow-growing fire ($\alpha=2.98 \text{ W/s}^2$) and a fast-growing fire ($\alpha=42.6 \text{ W/s}^2$). Upon activation of the fifth sensor the inversion algorithm has sufficient information to locate the fire. The slow-growing fire is seen to be located in three minutes and the fast-growing fire within one minute.

Figures 2a and b demonstrate the effect of random errors and systematic errors on the inversion algorithm's accuracy in predicting fire location. Results for both slow-growing and fast-growing fires are given. Location error is reported as the distance between predicted and actual fire locations, given in centimeters. The effect of random error is shown in Fig. 2a. In that figure, where no systematic error has been added (LAVENT is assumed to be a "perfect" fire model), pdf's for simulations of fires with no random error ($\sigma=0 \text{ sec}$) or moderate random error ($\sigma=5 \text{ sec}$), are given. Figure 2b shows the effect of systematic or model error on the accuracy of the inversion algorithm to predict the fire location. Pdf's are given for fire data with an added random error with $\sigma=5\text{s}$ for cases of systematic error corresponding to $a=0\text{s}$, $a=40\text{s}$, $b=0$, and $b=0.6$.

Errors in location predictions by the inverse problem solution algorithm are seen to be much more sensitive to random errors in fire data than to systematic errors in the fire model. This conclusion can be seen more clearly in Figs 3a and 3b where results for fast-growing fires are given. In Figs. 3a and b both the median location error and 95% confidence intervals about the median error are plotted versus random error standard deviation, σ . The 95% confidence interval represents a location error greater than the location errors for 95% or 950 out of 1000 fires in a test run. In Fig. 3a location error is plotted for three cases of systematic error: $a=0, 20, 40 \text{ sec}$ with $b=0.0$ while in Fig, 3b location error is plotted for three other cases of systematic error: $a=0 \text{ sec}$ with $b=0, 0.2, 0.4$.

In both figures varying systematic error by varying the parameters a and b has little effect on either the median or the 95% confidence intervals for location errors. On the other hand, increasing the random error standard deviation, σ , causes monotonic increases in both the inversion algorithm's median location error and 95% confidence interval.

Figures 4a and b demonstrate the effect of random and systematic errors on the accuracy of the inversion algorithm to predict the fire heat release rate for fast and slow-growing fires. Heat release rate error is reported as the ratio of heat release rate predicted by the inversion algorithm, divided by the actual fire's heat release rate, at the time of the fifth sensor activation. The effect of random error is shown in Fig. 4a where pdf's are given for fire data with $\sigma=0$ and 5 sec with no systematic error. The effect of systematic error is shown in Fig. 4b where pdf's are

given for fire data with added random error with $\sigma=5s$ and cases of systematic error corresponding to $a=0s$, $a=40s$, $b=0$, and $b=0.6$.

Figures 5 a and b show the large errors in heat release rate predictions that systematic errors in the fire model used in the inversion algorithm can lead to. Results given are for fast-growing fires only. Predicted heat release rate is seen to drop monotonically below actual heat release rate as either parameter a or b increases. Random errors can be seen to have little effect on the median heat release rate error, although larger random errors do cause the 95% confidence intervals on heat release rate error to spread substantially.

Some preliminary tests of the prototype fire detection system have been made. Twenty tests were run, in which a gas fueled camp stove (which produced about 2 kW thermal) was ignited and then placed in the model enclosure. The location and heat release rate of the flame source as determined by the prototype fire detection system were compared against the actual location and heat release rate of the flame source. Figures 6 a and b show the results of these comparisons. The figures give pdf's for location error (Fig. 6a) and heat release rate error (Fig. 6b). Figure 6 a shows that the prototype system was able to locate the flame source within a radius of 45 cm in all twenty tests. Figure 6 b shows that the prototype system was able to determine the flame source's heat release rate to within a factor of two for most test cases. For a few cases the prototype system was unable to determine a value for the flame source's heat release rate. Those cases are indicated in the figure as having $Q_{pred}/Q_{act} = 0.0$.

Acknowledgments

This work has been supported by the Building and Fire Research Laboratory of NIST through contract number 60NANB2D1290. The efforts of B. Munk in developing the inverse problem solution algorithm, J. Valler in the design of the prototype system, A. Bakkom in setting up the system, and T. Ribail in testing the system are acknowledged. The generous advice of L.Y. Cooper in the use of LAVENT is also gratefully acknowledge.

References

1. Ozisik, N.M., *Heat Conduction*, 2nd edition, John Wiley & Sons, Inc., New York, pp.571-616, 1993.
2. Heskestad, G., "Engineering relations for fire plumes," *Society of Fire Protection Engineers*, Technology report 82-8, 1982.
3. Cooper, L.Y., "Estimating the environment and response of sprinkler links in compartment fires with draft curtains and fusible link-actuated ceiling vents-theory," *Fire Safety Journal*, **16**, pp. 137-163 1990.
4. Bakkom, A.W., Richards, R.F., and Plumb, O.A., "Design of a prototype video-based fire detection system," NIST Annual Conference on Fire Research, Gaithersburg, MD, 1994.

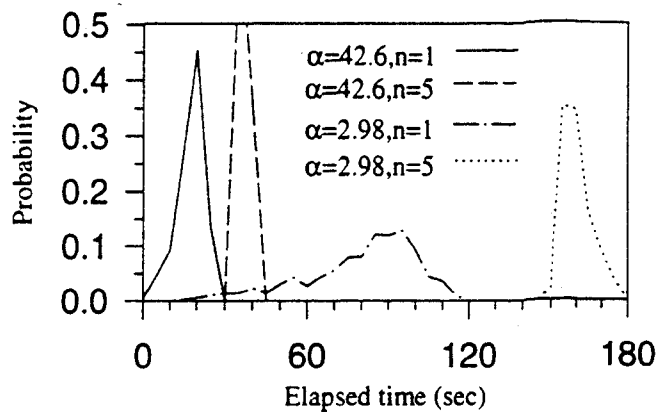


Fig. 1 PDF's for time to activation of first and fifth sensors

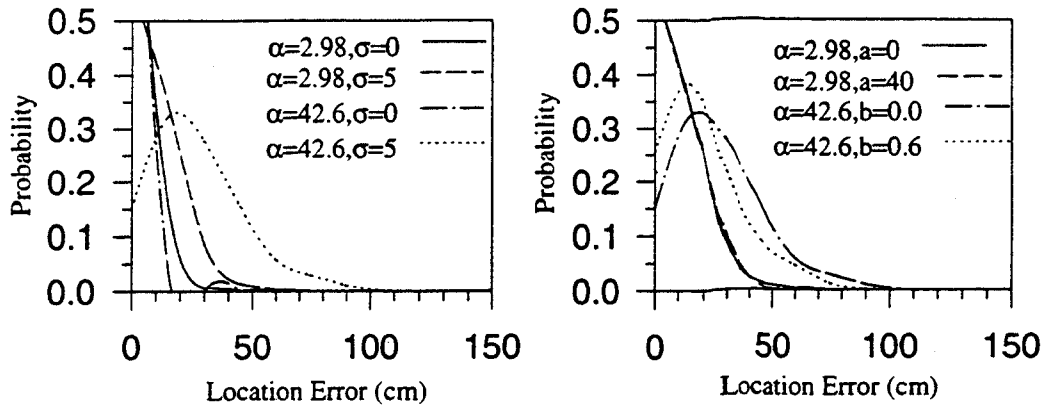


Fig. 2a,b Location error PDF's for various levels of random and systematic error. (Fig. 2a: $\sigma = 0,5s$; Fig.2b: $a = 0,40s, b = 0$ & $a = 0s, b = 0,0.6$)

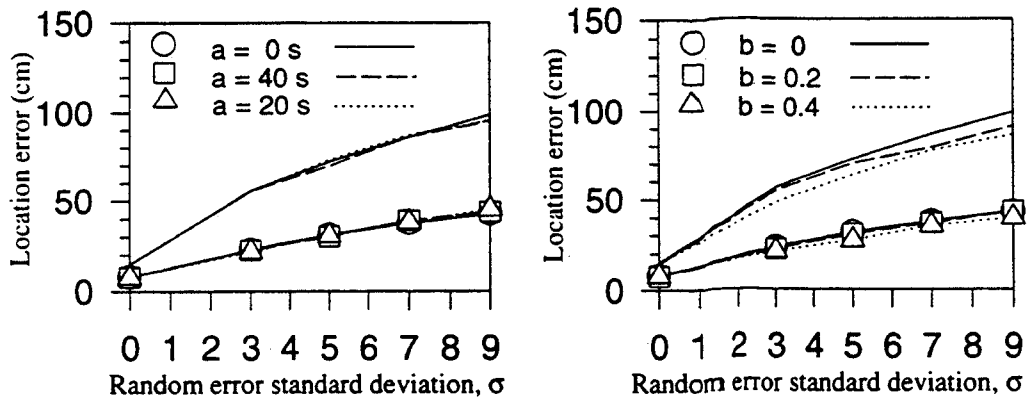


Fig. 3a,b Median location error with 95% confidence interval versus random error standard deviation, σ (Fig. 3a: $a = 0,20,40s, b = 0$; Fig.3b: $a = 0s, b = 0,0.2,0.4$).

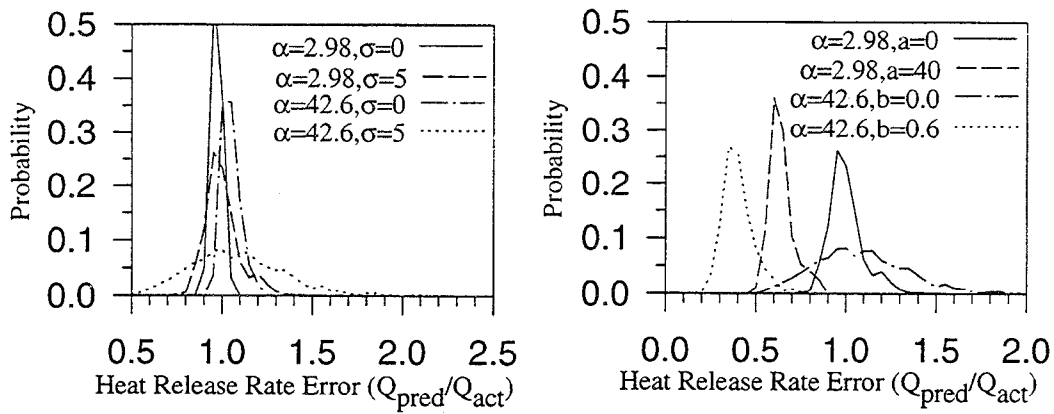


Fig. 4a,b Heat release rate error PDF's for various levels of random and systematic error. (Fig.4a: $\sigma = 0,5s$; Fig.4b: $a = 0,40s$; $b = 0$ & $a = 0s$; $b = 0.0,0.6$)

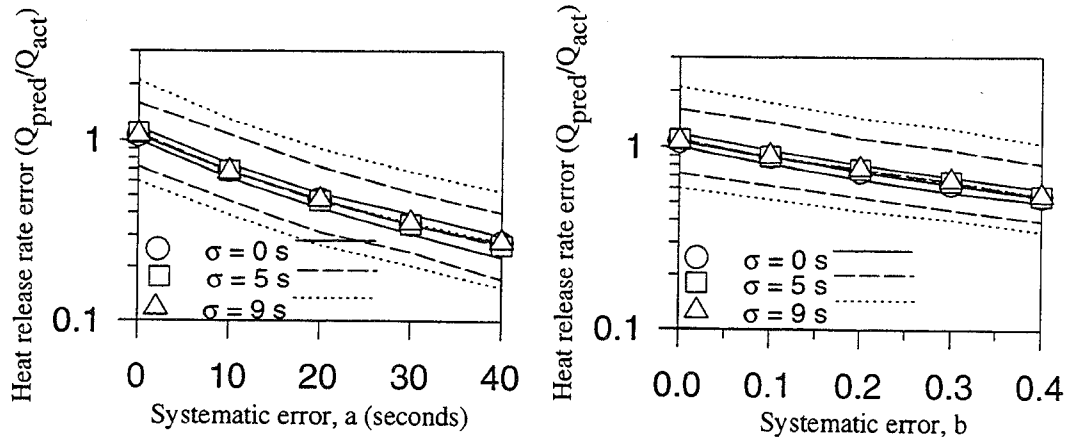


Fig. 5a,b Median heat rate error with 95% confidence intervals versus systematic error. (Fig.5a: $b = 0, \sigma = 0,5,9s$; Fig.5b: $a = 0, \sigma = 0,5,9s$).

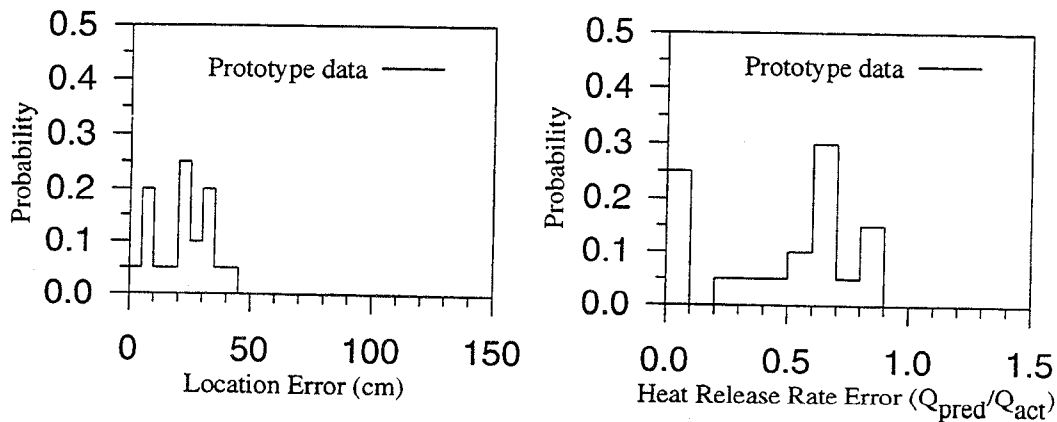


Fig. 6a,b Location and heat release rate error PDF's determined experimentally for the prototype fire detection system.